NEW METHOD FOR RESOLVING THE 180° AMBIGUITY IN SOLAR VECTOR MAGNETOGRAMS

Y.-J. MOON[1,2], HAIMIN WANG[1], THOMAS J. SPIROCK[1], P. R. GOODE[1] and Y. D. PARK[2]

[1] *Big Bear Solar Observatory, NJIT, 40386 North Shore Lane, Big Bear City, CA 92314 (yjmoon@bbso.njit.edu)*

[2] *Korea Astronomy Observatory, Whaamdong, Yuseong-gu, Daejeon, 305-348, Korea*

(Received ; Accepted 2003)

Abstract. We present a new method to resolve the 180° ambiguity for solar vector magnetogram measurements. The basic assumption is that the magnetic shear angle ($\Delta\theta$), which is defined as the difference between the azimuth components of observed and potential fields, approximately follows a normal distribution. The new method is composed of three-steps. First, we apply the potential field method to determine the azimuthal components of the observed magnetic fields. Second, we resolve the ambiguity with a new criterion: $-90° + \Delta\theta_{mp} \leq \Delta\theta \leq 90° + \Delta\theta_{mp}$, where $\Delta\theta_{mp}$ is the most probable value of magnetic shear angle from its number distribution. Finally, to remove some localized field discontinuities, we use the criterion: $\mathbf{B}_t \cdot \mathbf{B}_{mt} \geq 0$, where $\mathbf{B}_t$ and $\mathbf{B}_{mt}$ are an observed transverse field and its mean value for a small surrounding region, respectively. For an illustration, we have applied the new ambiguity removal method (Uniform Shear Method) to a vector magnetogram which covers a highly sheared region near the polarity inversion line of NOAA AR 0039. As a result, we have found that the new ambiguity solution was successful and removed spatial discontinuities in the transverse vector fields produced in the magnetogram by the potential field method. It is also found that our solution to the ambiguity gives nearly the same results, for highly sheared vector magnetograms and vertical current density distributions, of NOAA AR 5747 and AR 6233 as those of other methods. The validity of the basic assumption for an approximate normal distribution is demonstrated by the number distributions of magnetic shear angle for the three active regions under consideration.

1. Introduction

When one analyzes vector magnetograms from solar magnetograph measurements, one of the most challenging problems is to resolve the 180° ambiguity in the azimuth of the observed transverse fields. This ambiguity is attributed to the fact that the two anti-parallel polarization signals of the transverse fields are identical to each other since the transverse measurements from the magnetograph provides only the plane of linear polarization. For all observed vector magnetograms, the ambiguity should be resolved to obtain the correct direction of the transverse vector fields. A reasonable method to solve this ambiguity

is of great importance because knowing the proper orientation of solar magnetic fields is required to gain a meaningful understanding of several physical quantities of flare producing active regions such as shear angle, vertical current density, magnetic free energy density and MAD (The Maximum Angular Difference between two adjacent field vectors, Moon *et al.*, 1999).

Hagyard *et al.* (1984) defined the magnetic shear angle as the angular difference between an observed transverse field and the transverse component of the potential field, which is computed by employing observed longitudinal fields as a boundary condition. That is, the magnetic shear angle $\Delta\theta$ is given by

$$\Delta\theta = \theta_o - \theta_p \,, \tag{1}$$

in which θ_o is the azimuth of the observed transverse field and θ_p is the azimuth of the corresponding potential field component. Noting that flares are associated with large magnetic shear of strong transverse fields, Wang (1992) proposed a transverse weighted mean shear angle given by

$$\Delta\overline{\theta} = \frac{\sum B_t \Delta\theta}{\sum B_t}, \tag{2}$$

where B_t is the transverse field strength and the sum is taken over all of the pixels under consideration. He found that the weighted mean shear angle of a flaring active region jumped about 5° coinciding with an X-class flare. He also showed that five additional X-class flares had the same pattern of shear angle variation (Wang *et al.*, 1994; Wang, 1997). Wang *et al.* (2002) reported on two X-class flares, in addition to the two papers mentioned previously, during which the shear increased.

However, the association of the shear of an active region with solar flares still remains controversial. There were apparently contrary reports that the shear may increase, decrease or remain the same after flares (Hagyard *et al.*, 1993; Ambastha *et al.*, 1993; Hagyard *et al.*, 1999). Chen *et al.* (1994) found that there were no detectable changes in magnetic shear after 18 M-class flares. Since the determination of the magnetic shear angle strongly depends on resolving the 180° ambiguity, it is very important to solve this problem.

To resolve the ambiguity, some constraints on the field azimuth are to be introduced in terms of theoretical and/or observational aspects (for review, Gary and Demoulin 1995). One of the commonly used techniques is the potential field method based on the fact that an observed transverse magnetic field tends not to deviate much from a tangential component of an associated potential field; that is, the direction of the transverse field is chosen such that the angular difference between the observed and the potential components makes an acute angle. However,

this criterion may break down for flaring active regions, which generally have strong shears near a polarity inversion line; that is, the transverse fields are often nearly parallel to the polarity inversion line.

More sophisticated and/or multi-step methods to resolve this ambiguity have been suggested by several authors. Canfield *et al.* (1993) employed a multi-step approach by using several criteria, which was well described in the appendix of their paper. The main step of their methodology is to choose the orientation of the transverse field which minimizes the angle between neighboring field vectors. This is accomplished by maximizing the sum of the vector dot product of the field vector with each of its adjacent eight neighbors. Then the orientation of the field is iteratively determined by minimizing the field divergence $|\nabla \cdot \mathbf{B}|$ in regions with strong total magnetic field strength ($\geq 1000G$) and a high degree of shear. Metcalf (1994) presented an elegant method which simultaneously minimizes both the divergence of the magnetic field and the electric current density using a simulated annealing algorithm. Gary and Demoulin (1995) developed a non-linear optimization approach which handles highly non-potential magnetic regions. These two methods are primarily concerned with the functional minimization of the total current density and/or the divergence of field vectors. The different types of methods used to resolve the ambiguity have been well discussed by several authors (e.g., Aly 1989, Sakurai 1989; Gary and Demoulin 1995; McClymont *et al.*, 1997). Determining which method is optimal is still difficult since it is impossible to obtain a magnetogram free from this ambiguity.

In this study, we present a relatively simple and objective method for resolving the 180° ambiguity using three steps. This method minimizes not only the statistical discontinuities in the number distribution of the magnetic shear angle but also spatial discontinuities by adjusting the direction of a transverse field to conform more closely with that of a mean transverse field for a surrounding local area. In Section 2, we propose a new method to resolve the 180° ambiguity and explain its procedure in detail. For convenience, we will hereafter refer to this new method as the Uniform Shear Method (USM). In Section 3, we illustrate the methodology using a vector magnetogram of NOAA AR 0039. In Section 4, the ambiguity-resolved vector fields and vertical current densities of NOAA AR 5747 and 6233, based on the USM for resolving the 180° ambiguity, are compared with those based on other methods. Finally, a brief summary and discussion is given in Section 5.

2. Methodology

The USM for resolving the 180° ambiguity in solar vector magnetograms is conceptually simple and is composed of three steps. Here we describe every step in detail.

2.1. First Step

For the case of a potential field, the magnetic field can be expressed as

$$\mathbf{B} = -\nabla\Phi, \tag{3}$$

where Φ is a scalar potential. Using $\nabla \cdot \mathbf{B} = 0$, the scalar potential should satisfy the Laplace equation:

$$\nabla^2\Phi = 0, \tag{4}$$

where an observable quantity B_z can be used as the boundary condition $B_z = \partial\Phi/\partial z$.

The potential field solution was initially suggested by Schmidt (1964) with the use of the Green function method. Later, the Fourier expansion method was employed by Teuber *et al.* (1977) and Sakurai (1989). For our study, we have used a Fourier expansion method. The criterion of this method is given by

$$-90^\circ \leq \theta_o - \theta_p \leq 90^\circ. \tag{5}$$

2.2. Second Step

This step is the main process of the USM. The basic assumption of the second step is that a plot of the actual magnetic shear angle ($\Delta\theta$) approximately follows a normal distribution characterized by a most probable value of $\Delta\theta_{mp}$. The validity of this assumption will be demonstrated in the next sections. Under this assumption, we suggest a new criterion given by

$$-90^\circ + \Delta\theta_{mp} \leq \theta_o - \theta_p \leq 90^\circ + \Delta\theta_{mp}. \tag{6}$$

In practice, $\Delta\theta_{mp}$ is determined as follows. First, the initial estimation is a shear angle at which the histogram of shear angle has its maximum value. Then, we apply the criterion given by Equation (6) to the vector magnetogram under consideration. Second, we make a gaussian fit to the histogram of the magnetic shear angle in order to determine our second estimation as a central position of the fit. Third, our final estimate is determined to be the shear angle which gives the maximum

pixel number in the range of $-80 + \Delta\theta_{mp}$ and $80 + \Delta\theta_{mp}$ by shifting the second estimation from -20 to 20 degrees. Here, the maximum pixel number corresponds to the minimum number of shear angles in both tails of the histogram. The final estimate is devised for active regions showing more complex shear angle distributions.

This second step minimizes the discontinuities in the number distribution of magnetic shear from a statistical point of view. This criterion is equivalent to the potential method if $\Delta\theta_{mp}$ is zero. For highly sheared magnetic fields, the sign of magnetic helicity may also be a criterion for resolving the 180° ambiguity; that is, $\Delta\theta > 0$ for positive helicity sign and $\Delta\theta < 0$ for negative helicity sign. This criterion is also equivalent to Equation (6) when $\Delta\theta_{mp}$ is $\pm 90°$. Thus, both the potential method and the helicity sign method are special cases of Equation (6).

The second step described here is conceptually similar to the second step of Canfield *et al.* (1993), in which they compute the linear (constant α) force-free field with α selected to match the non-potentialities estimated by the potential method and then select the orientation of the transverse field which gives the closest match to the force-free field. However, our approach differs from their method in two aspects. First, we do not assume a specific type of field configuration, such as a linear-force free field. The linear force-free field is governed by the same Helmholtz equation that describes electromagnetic radiation produced by oscillating sources in the photosphere (McClymont *et al.*, 1997). In addition, the solution of the Helmholtz equation has some non-uniqueness problems, as well as the condition for finite energy (Alissandrakis, 1981). Second, Moon *et al.* (2002a) noted that there are some systematic differences between the linear force-free coefficients obtained from the following two methods: (1) the least square method between vertical current density and vertical magnetic field, and (2) the minimized difference between transverse components of linear force-free models with different constant α and observed transverse fields. This difference also depends on the force-freeness of magnetic fields at the photosphere.

2.3. Third Step

Finally, we propose an objective criterion given by

$$\mathbf{B_{ot}} \cdot \mathbf{B_{mt}} > 0, \tag{7}$$

where $\mathbf{B_{ot}}$ is an observed transverse vector field and $\mathbf{B_{mt}}$ is a mean transverse vector given by

$$\mathbf{B_{mt}}(i,j) = B_{mx}\hat{\mathbf{x}} + B_{my}\hat{\mathbf{y}}, \tag{8}$$

where B_{mx} and B_{my} are mean field strengths of the x and y components for a surrounding local area $(i-w : i+w, j-w : j+w)$, respectively. This process makes the direction of an observed transverse field conform to a mean transverse field for a surrounding local area, which is conceptually similar to Aly (1989) and Canfield *et al.* (1993) who both employed partially interactive methods to minimize the inner product between a transverse field and its adjacent vector. This is expected to reduce some localized magnetic field discontinuities as well as mis-determinations due to observational errors.

After the removal of the 180° ambiguity, one may want to rotate vector fields to the heliographic coordinate system (Gary and Hagyard, 1990). If an active region is far from the disk center, the resulting heliographic field would be highly sensitive to the azimuthal ambiguity since the errors caused by the ambiguity of the vector fields are compound with the projection effect and/or the geometric curvature, as Gary and Hagyard (1990) have noted. Thus, we are reluctant to transform the coordinates unless the active region is near the disk center.

3. Illustration

To illustrate the USM, we have used a vector magnetogram of NOAA AR 0039 for which Wang et al.(in preparation) showed that there was an abrupt shear change associated with the M8.7 flare on July 26, 2002. This magnetogram was taken with the Digital Vector Magnetograph (DVMG) at Big Bear Solar Observatory (BBSO). A detailed description of the instrument, and the data analysis procedure, is found in Spirock *et al.* (2002) and Moon *et al.* (2002b).

Figure 1 shows the number distribution of the magnetic shear angle from a magnetogram of NOAA AR 0039 observed at 18:40 UT on July 26, 2002. The three figures (from top to bottom) correspond to the three steps of the USM, respectively. They illustrate the basic assumptions and methodology of the present approach. In the first step (top panel), the number distribution of the magnetic shear angle, based on the potential field method, has two local maxima, which are widely separated ($-90°$ and 70°). However, these two maxima are integrated into a single maximum during the second step (middle panel). This implies that the local maximum at $-90°$ in the first step originated from the potential field method. Also, note that the number distribution of the magnetic shear angle, as a result of the second step, closely follows a normal distribution with a most probable value of approximately 70°. Such a normal distribution demonstrates that our assumption for the second step, as described in Section 2, is valid for this magnetogram. It is also

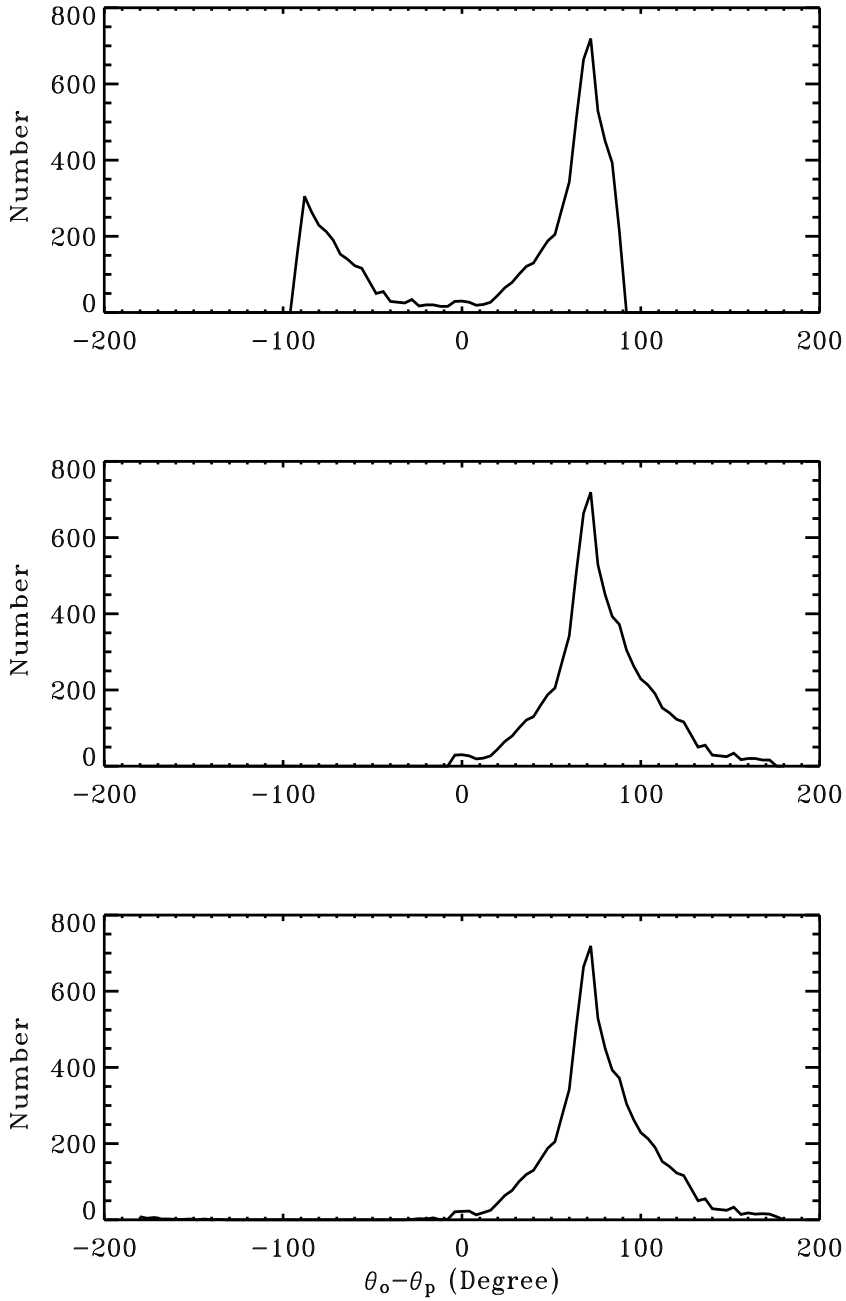

Figure 1. Variation of the number distribution of magnetic shear angle ($\theta_o - \theta_p$) for the three steps: the first step (the potential method; top panel), the second step (middle panel), and the third step (bottom panel).

noted that two critical values ($-90° + \Delta\theta_{mp}$ and $90° + \Delta\theta_{mp}$) in the second criterion are located at both tails of the number distribution of magnetic shear angle. This fact indicates that our second step is a minimization process of the discontinuities in the number distribution of magnetic shear angle from a statistical point of view. It is also found that the number distribution of the magnetic shear angle, from the second step to the third step, has changed little, which may be attributed to the fact that most of the spatial discontinuities are already removed by the second step.

Figure 2 shows a comparison of the vector fields for the magnetogram used in Figure 1, from each of the three steps. Our area of interest is the highly sheared region near the polarity inversion line. As can be seen in figures, the direction of the transverse field is nearly parallel to the polarity inversion line. It is evident that there are noticeable differences between the results of steps one and two in the area of negative polarity. Note that while the vector magnetogram based on the potential method have numerous discontinuities in the transverse vector fields, the magnetogram in the second step does not. It seems that the local discontinuities in the upper panel of Figure 2 are associated with the two local maxima seen in the top panel of Figure 1; that is, the local discontinuities are due to a result of the criteria in the potential field method. The middle panel in Figure 2 shows two mis-determinations around (38,7) and (46,5), which might be due to Zeeman saturation of the filter-based magnetograms in sunspot umbrae. However, these mis-determinations are removed in the third step, as seen in the bottom panel of Figure 2.

4. COMPARISON WITH OTHER METHODS

To compare the USM for resolving the 180° ambiguity with other methods, we consider vector magnetograms of two active regions: NOAA AR 5747 (S26W07) at 17:41 UT on October 20, 1989, and NOAA 6233 (N13W02) at 21:56 UT on August 29, 1990. These magnetograms obtained by the Mees Solar Observatory (MSO) were chosen since they show strong shear along the neutral lines. In addition, they were already used for observational studies of photospheric magnetic vector fields and vertical current density distributions. AR 5747 was used for an observational test of the method to correct the ambiguity based on the minimum energy solution (Metcalf, 1994) and for an examination of several physical characteristics: vertical current density (Leka *et al.*, 1993), non-potential parameters (Moon *et al.*, 2000), and force-free characteristics (Moon *et al.*, 2002a). AR 6233 was also used for

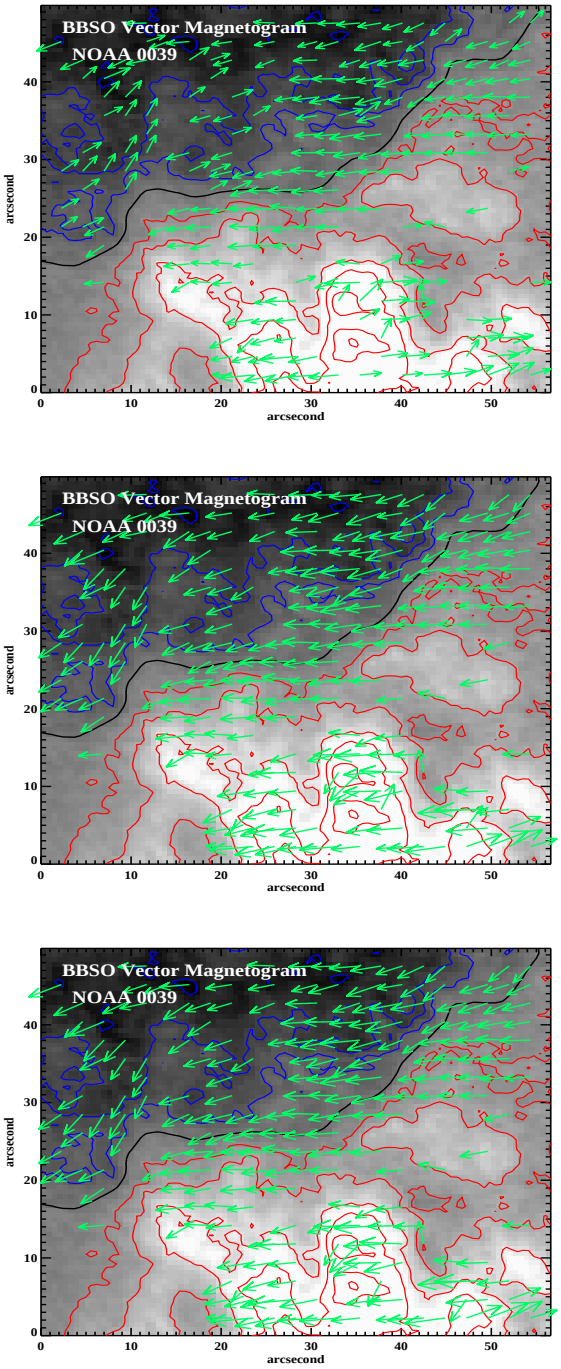

Figure 2. Ambiguity-resolved vector magnetograms in three steps: the first step (top panel), the second step (middle panel), and the final step (bottom panel). Red (blue) contours correspond to positive (negative) polarity. Arrows indicate the transverse fields. The black line corresponds to the polarity inversion line.

studies of vertical current distribution (de la Beaujardiere *et al.*, 1993) and its force-freeness (Moon *et al.*, 2002a). Most of the data analyzing procedure is well described in Canfield *et al.* (1993) and Moon *et al.* (2002a). Using these data sets, we will compare the USM to solve the 180° ambiguity with the muti-step ambiguity method of Canfield *et al.* (1993).

The magnetograms which have been corrected for the 180° ambiguity, in addition to the corresponding vertical density maps, are presented in Figures 3 and 4. The figures indicate that the two methods produce quite similar results, in both vector fields and vertical density distributions. Metcalf (1994) has previously shown that vector fields that have had the ambiguity corrected by his minimum energy method are similar to those based on the multi-step method of Canfield *et al.* (1993). As seen in Figures 5 and 6, the vector fields of AR 6233, and the corresponding vertical density distributions from both ambiguity solutions, are quite similar to each other. Even though there are four polarity inversion lines having some different shearing patterns, it seems that the USM has worked quite well.

Figure 7 shows the number distributions of the magnetic shear angles for the two active regions under consideration. In addition to the bottom panel of Figure 1, the two distributions in Figure 7 approximately follow normal distributions, which are additional demonstrations for the validity of the basic assumption given in the second step.

5. SUMMARY AND DISCUSSION

In this paper, we propose a new method, which we refer to as the Uniform Shear Method (USM), for resolving the 180° ambiguity in solar vector magnetograms. The new solution is composed of the following three-steps: (1) the potential method, (2) a second criterion given by $-90^\circ + \Delta\theta_{mp} \leq \theta_o - \theta_p \leq 90^\circ + \Delta\theta_{mp}$, and (3) a third criterion: $\mathbf{B}_t \cdot \mathbf{B}_{mt} \geq 0$. This method is proposed for minimizing some discontinuities in the number distribution of the magnetic shear angle by the second step as well as some spatial discontinuities of observed transverse fields by the third step. We have applied the USM to a vector magnetogram of NOAA AR 0039 and found that the USM has removed many of the spatial discontinuities seen in the magnetogram based on the potential method. In addition, we have shown that two different ambiguity solutions (Canfield *et al.*, 1993 and the USM) produce nearly the same results for highly sheared vector magnetograms of active regions AR 5747 and AR 6233.

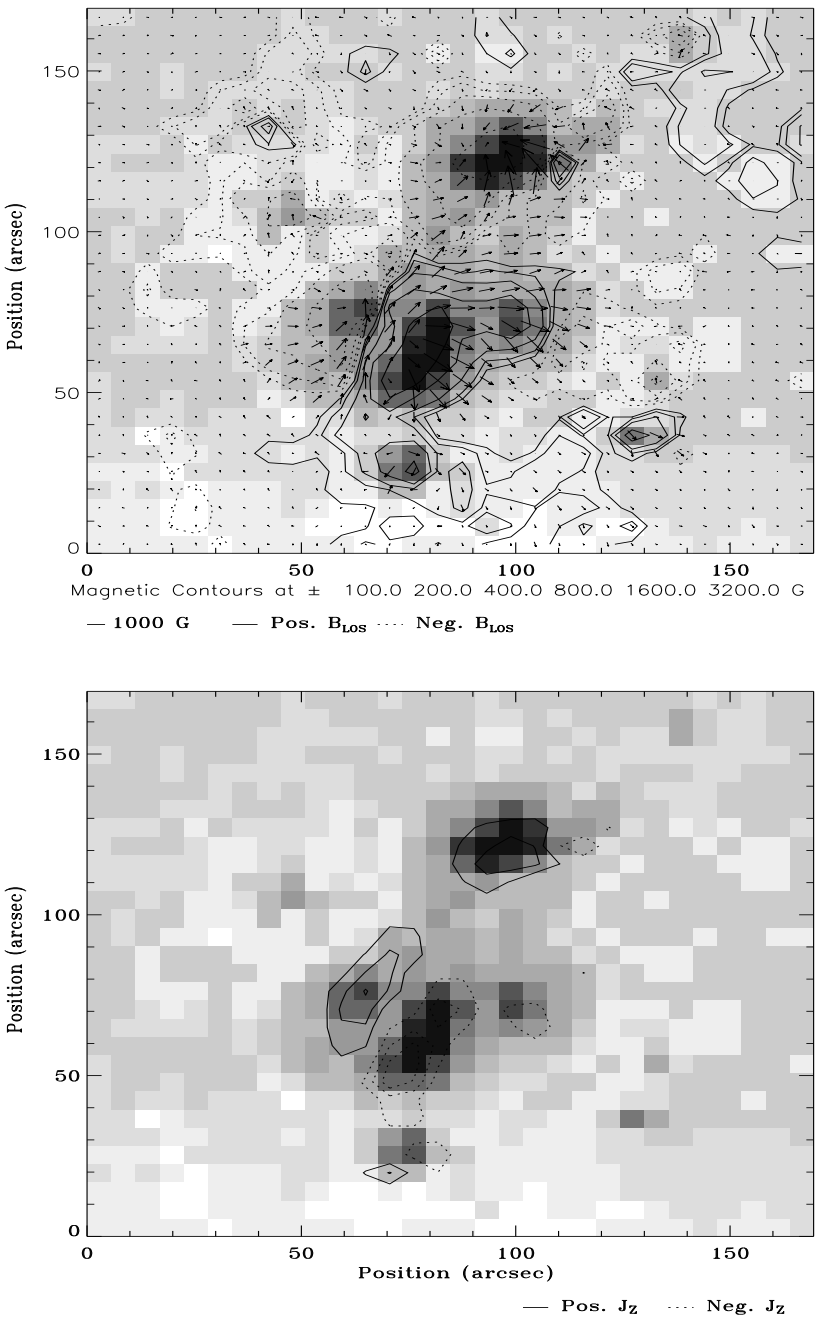

Figure 3. MSO vector magnetogram (upper panel) of AR 5747 based on the multi-step ambiguity removal method of Canfield *et al.* (1993) and the corresponding vertical current density map (lower panel), which are superposed on the white light image taken on Oct. 20, 1989. The contour levels in the lower panel are 5, 10, 15, and 20 mA/m^2, respectively.

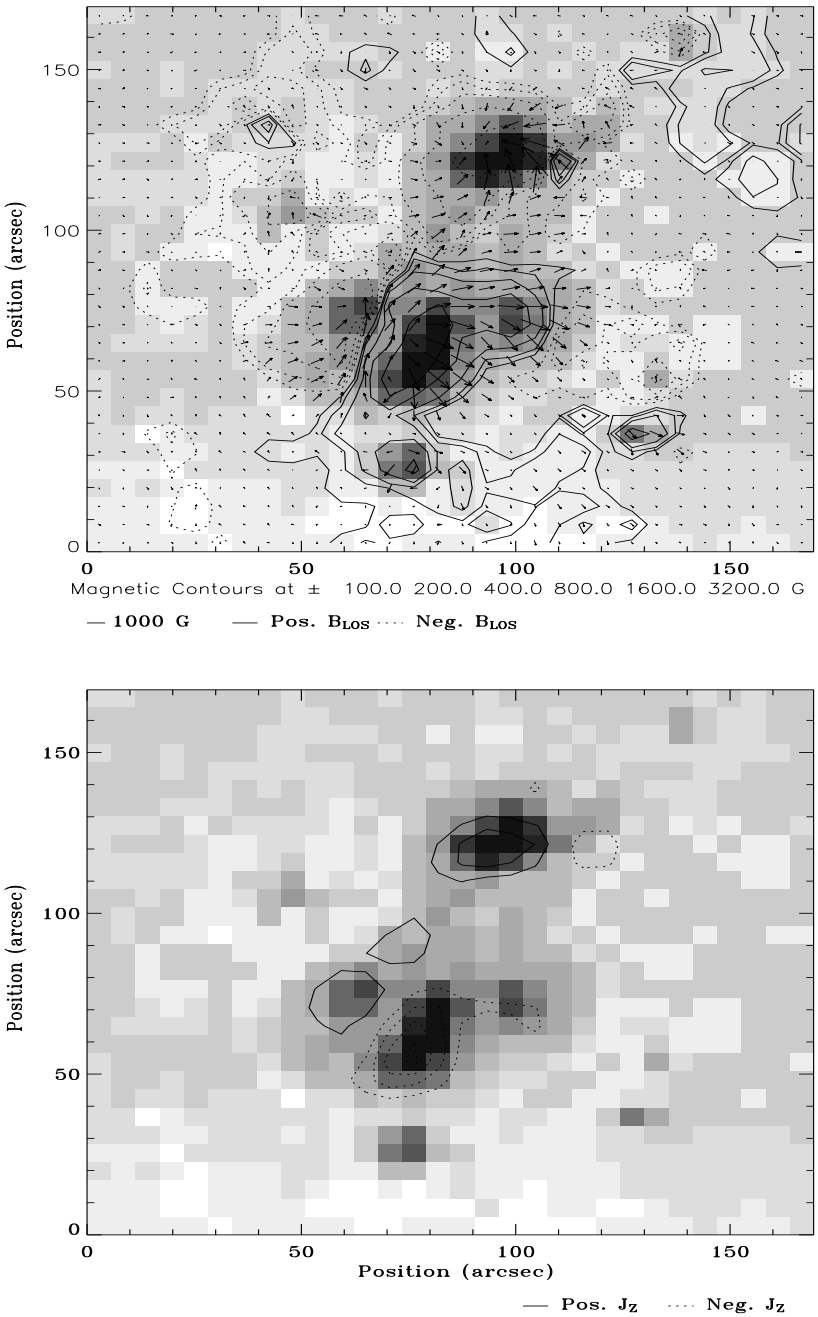

Figure 4. MSO vector magnetogram (upper panel) of AR 5747 based on the USM and the corresponding vertical current density map (lower panel). Additional information is the same as that found for Figure 3.

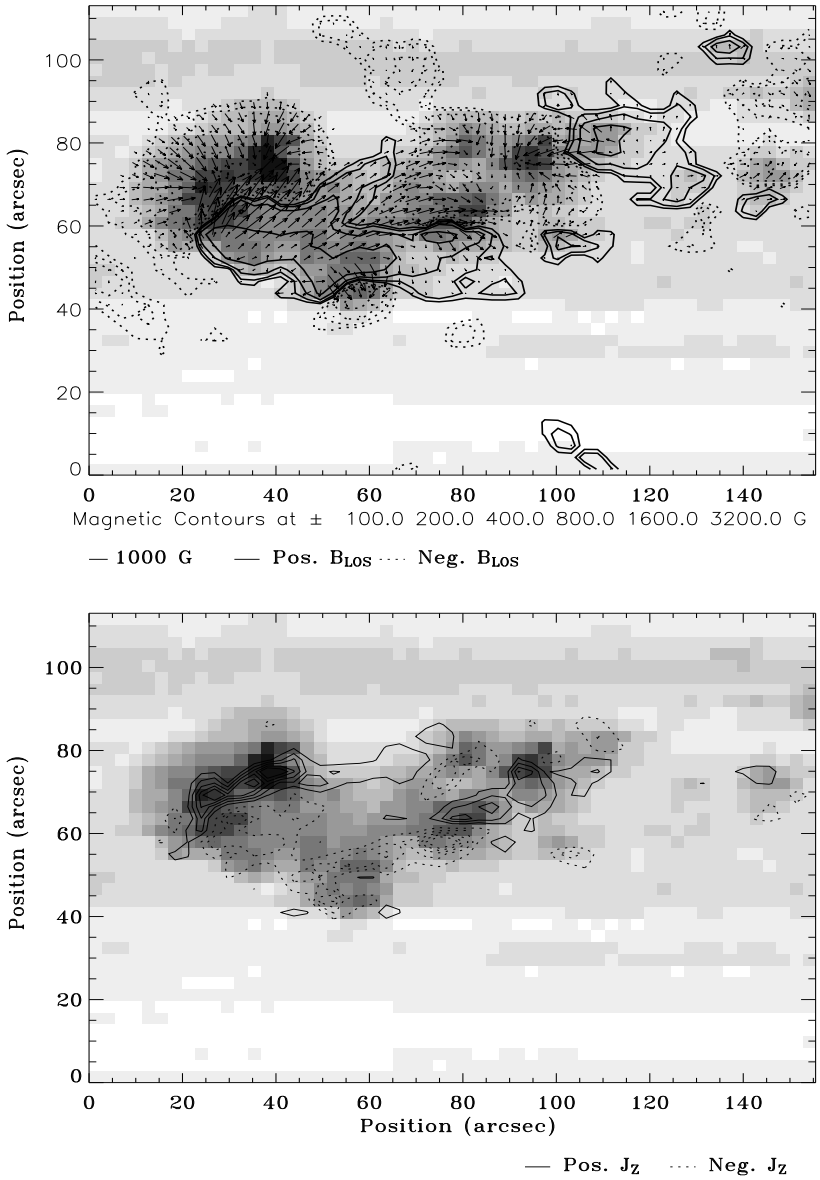

Figure 5. MSO vector magnetogram (upper panel) of AR 6233 based on the multi-step ambiguity removal method of Canfield *et al.*(1993) and the corresponding vertical current density map (lower panel), which are superposed on the white light image taken on Aug. 29, 1990. Additional information is the same as that found for Figure 3.

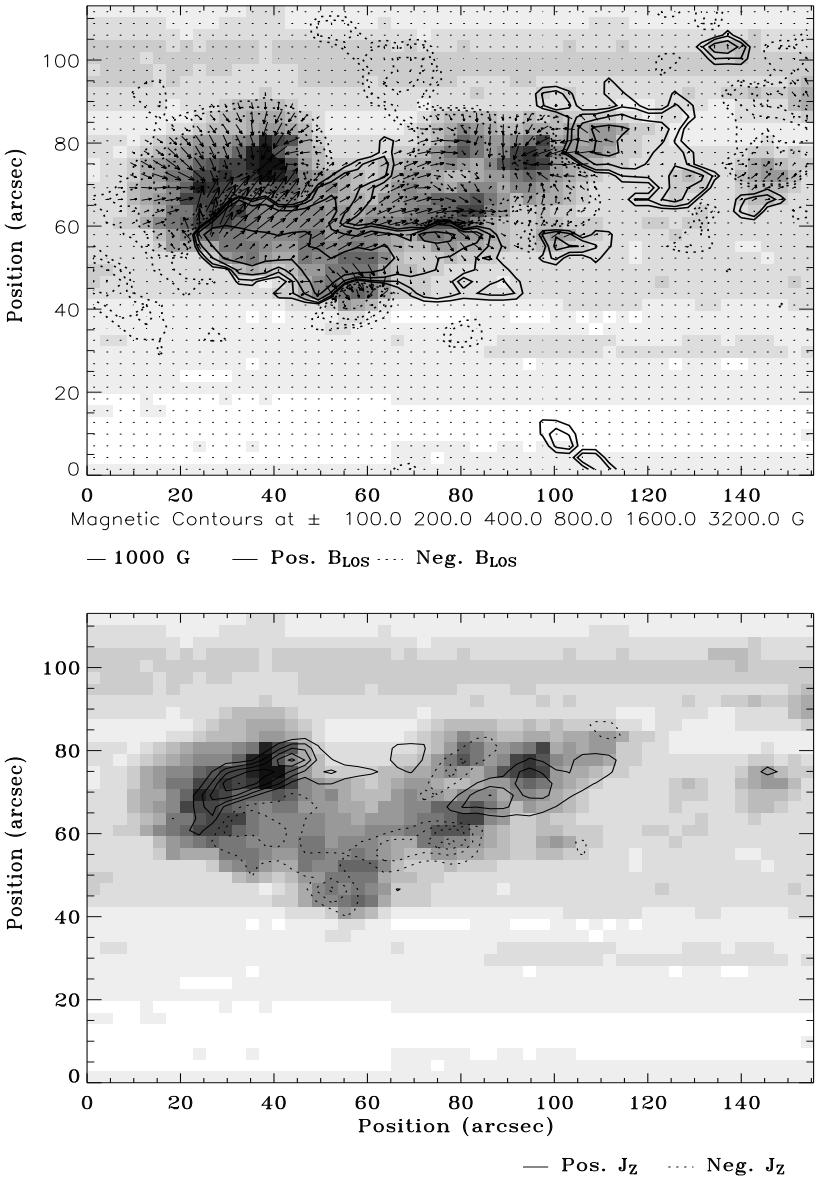

Figure 6. MSO vector magnetogram (upper panel) of AR 6233 based on the USM and the corresponding vertical current density map (lower panel). Additional information is the same as that found for Figure 3.

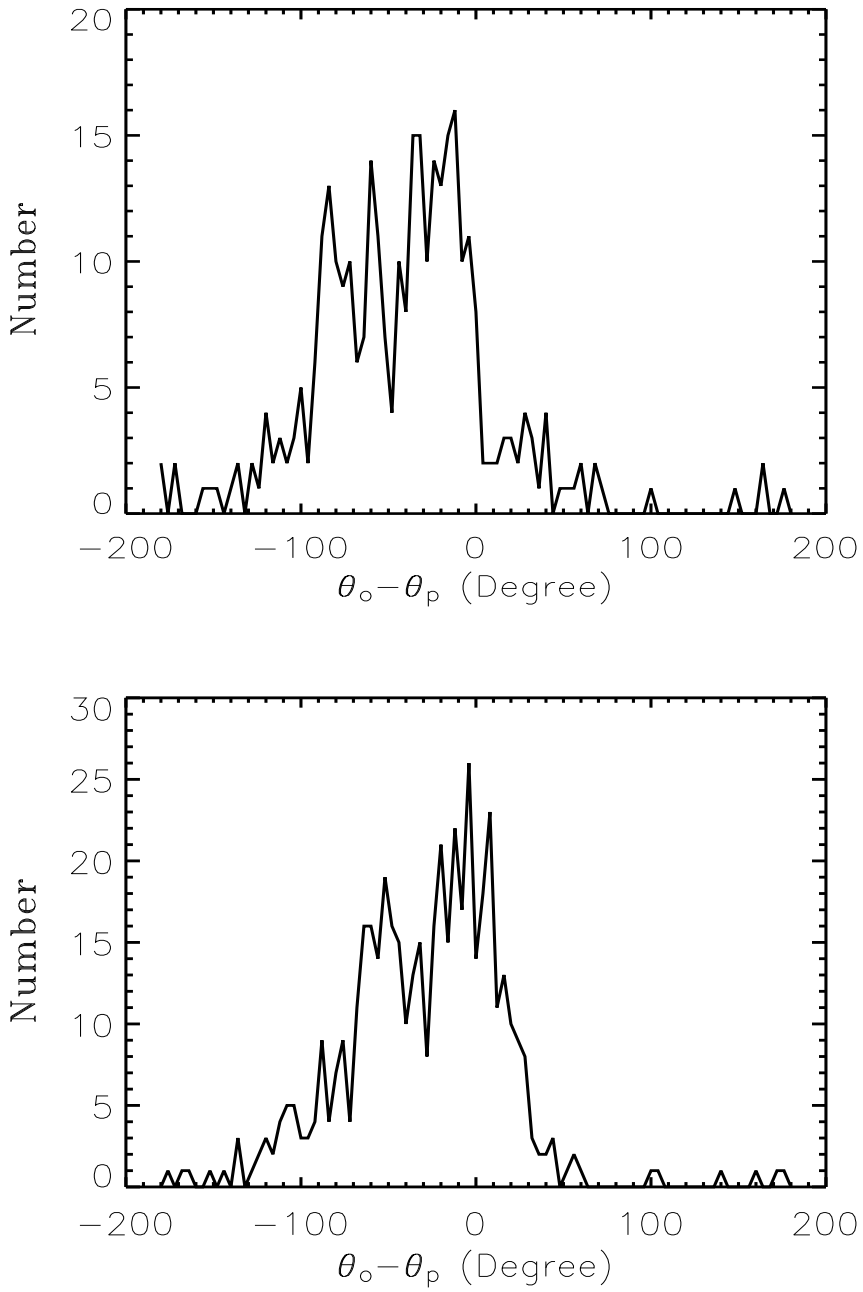

Figure 7. Number distributions of the magnetic shear angles ($\theta_o - \theta_p$) for AR 5747 (upper panel) and AR 6233 (lower panel).

Finally, we will now discuss some advantages and disadvantages of the present approach. The major assumption of the USM is that the number distribution of the magnetic shear angle approximately follows a normal distribution, whose validity has been demonstrated for the three active regions under consideration. Thus, this assumption has at least an empirical basis. From observational and theoretical points of view, shearing patterns of photospheric magnetic fields, which are connected to overlying fields, are expected to be rather uniform near the polarity inversion line when one considers that there is a flux rope above the polarity inversion line. This characteristics make it possible to minimize the discontinuities in transverse vector fields from a statistical point of view. In addition, the USM is relatively simple and can be made in nearly objective ways.

However, some active regions may have very complex distributions of magnetic shear (or quite different values of linear fore-free coefficient). In this case, the USM may not be effective for a whole area showing complex structures but for the region of interest having a relatively uniform shearing pattern. In addition, there may be a concern if the discontinuities are so numerous that the number distributions of shear angle have two nearly equal peaks. Thus, we suggest plotting the number distribution of the magnetic shear angle for the entire area, or some local area, when applying the USM to magnetogram data. By manually inspecting the plot, one may find a criterion for the second step of the USM so that statistical discontinuities in the number distribution of magnetic shear angle can be minimized, even in the case that there are multiple peaks in the distribution. In complicated cases such as this, it may be necessary to have a procedure to interactively determine θ_{mp} and/or to manually select a desirable region of interest. Noting that the USM was successfully applied to the entire area of two flare-productive active regions in Section 4, without any interactive procedures, we think that these cases are rare.

Acknowledgements

We greatly appreciate the referee's constructive comments. We are very thankful to the BBSO observing staff for obtaining the data. We thank Dr. J. Qiu and Dr. T. Metcalf for providing us with data analysis programs. This work has been supported by NASA grants NAG5-10894, NAG5-7837, and NAG 5-12782, by NSF-ATM-0086999, by a MURI grant of AFOSR, by the US-Korea Cooperative Science Program (NSF INT-98-16267), and by a NRL grant M10104000059-01J000002500 of the Korean government.

References

Alissandrakis, C. E.: 1981, *Astron. and Astrophys.* **100**, 197.

Ambastha, A., Hagyard, M.J., and West, E. A.: 1993, *Solar Phys.* **148**, 277.

Aly, J. J. 1989, *Solar Phys.* **120**, 19.

de La Beaujardiere, J.-F., Canfield, R. C., and Leka, K. D. 1993, *Astrophys. J.* **411**, 378.

Canfield, R. C., de La Beaujardiere, J.-F., Fan, Y., Leka, K. D., McClymont, A. N., Metcalf, T. R., Mickey, D. L., Wuelser, J.-P., and Lites, B. 1993, *Astrophys. J.* **411**, 362.

Chen, J., Wang, H., Zirin, H., and Guoxiang, A.: 1994, *Solar Phys.* **154**, 261.

Gary, G. A. and Hagyard, M. J: 1990, *Solar Phys.* **126**, 21.

Gary, G. A. and Demoulin, P.: 1995, *Astrophys. J.* **445**, 982.

Hagyard, M. J., Smith, Jr, J. B., Teuber, D., and West, E. A.: 1984, *Solar Phys.* **91**, 115.

Hagyard, M. J., West, E. A., and Smith, J. E.: 1993, *Solar Phys.* **144**, 141.

Hagyard, M. J., Stark, B. A., and Venkatakrishnan, P.: 1999, *Solar Phys.* **184**, 133.

Leka, K. D., Canfield, R. C., McClymont, A. N., de la Beaujardiere, J. F., and Fan, Y.: 1993, *Astrophys. J.* **411**, 370.

McClymont, A. N., Jiao, L., and Mikić, Z.: 1997, *Solar Phys.* **174**, 191.

Metcalf, T. R.: 1994, *Solar Phys.* **155**, 235.

Moon, Y.-J., Yun, H. S., Lee, S. W., Kim, J.-H., Choe, G. S., Park, Y. D., Ai, G., Zhang, H. Q., Fang, C. 1999, *Solar Phys.* **184**, 323.

Moon, Y.-J., Yun, H. S., Choe, G. S., Park, Y. D., and Mickey, D. L.: 2000, *J. Korean Astron. Soc.* **33**, 63.

Moon, Y.-J., Choe, G. S., Yun, H. S., Park, Y. D., and Mickey, D. L.: 2002a, *Astrophys. J.* **568**, 422.

Moon, Y.-J., Wang, H., Spirock, T., and Park, Y. D.: 2002b, *J. Korean Ast. Soc.* **35**, 143.

Sakurai, T.: 1989, *Space Science Rev.* **51**, 1.

Schmidt, H. U. 1964, in *Phys. of Solar Flares,* ed. W.N. Hess, NASA SP-50, p107.

Spirock, T. J., Yurchyshyn, V. B., and Wang, H.: 2002, *Astrophys. J.* **572**, 1072.

Teuber, D., Tanderberg-Hanssen, E., and Hagyard, M. J.: 1977, *Solar Phys.* **53**, 97.

Wang, H.: 1992, *Solar Phys.* **140**, 85.

Wang, H., Ewell, M. W., Jr., Zirin, H., and Ai, G.: 1994, *Astrophys. J.* **424**, 436.

Wang, H.: 1997, *Solar Phys.* **174**, 163.

Wang, H., Spirock, T. J., Qiu, J., Ji, H., Yurchyshyn, V. B., Moon, Y.-J., Denker, C., and Goode, P. R. 2002, *Astrophys. J.* **576**, 497.